



Published in final edited form as:

Oncogene. 2011 January 27; 30(4): 410–422. doi:10.1038/onc.2010.454.

Mitogenic Sonic hedgehog signaling drives E2F1-dependent lipogenesis in progenitor cells and Medulloblastoma

Bobby Bhatia², Michael Hsieh¹, Anna Marie Kenney², and Zaher Nahlé^{1,*}

¹Department of Cardiothoracic Surgery, Weill Cornell Medical College, New York, NY 10021

²Department of Cancer Biology and Genetics, Memorial Sloan-Kettering Cancer Center, New York NY 10021

Abstract

Deregulation of the Rb/E2F tumor suppressor complex and aberration of Sonic hedgehog (Shh) signaling are documented across the spectrum of human malignancies. Exaggerated *de novo* lipid synthesis is also found in certain highly proliferative, aggressive tumors. Here, we show that in Shh-driven medulloblastomas, Rb is inactivated and E2F1 is up-regulated, promoting lipogenesis. Extensive lipid accumulation and elevated levels of the lipogenic enzyme FASN mark those tumors. In primary cerebellar granule neuron precursors (CGNPs), proposed Shh-associated medulloblastoma cells-of-origin, Shh signaling triggers E2F1 and FASN expression while suppressing fatty acid oxidation (FAO), in a Smoothened-dependent manner. In the developing cerebellum, E2F1 and FASN co-localize in proliferating CGNPs. *In vivo* and *in vitro*, E2F1 is required for FASN expression and CGNP proliferation, and E2F1 knockdown impairs Shh-mediated FAO inhibition. Pharmacologic blockade of Rb inactivation and/or lipogenesis inhibits CGNP proliferation, drives medulloblastoma cell death, and extends survival of medulloblastoma-bearing animals *in vivo*. These findings identify a novel mechanism through which Shh signaling links cell cycle progression to lipid synthesis, through E2F1-dependent regulation of lipogenic enzymes. These findings pertinent to the etiology of tumor metabolism also underscore the key role of the Shh→E2F1→FASN axis in regulating *de novo* lipid synthesis in cancers, and as such its value as a global therapeutic target in hedgehog-dependent and/or Rb-inactivated tumors.

Keywords

cerebellum; sonic hedgehog; medulloblastoma; E2F1; Rb; metabolism; lipogenesis; cell cycle; cancer

Users may view, print, copy, download and text and data- mine the content in such documents, for the purposes of academic research, subject always to the full Conditions of use: http://www.nature.com/authors/editorial_policies/license.html#terms

*Corresponding author: zan2003@med.cornell.edu Tel 212-746-9450; fax 212-746-9393.

Conflict of Interest

The authors have no competing financial interests in relation to this work.

Introduction

The Hedgehog (Hh) family of mitogens/morphogens plays a pleiotropic role in cell fate determination, organ patterning, and expansion of progenitor cell populations (Wechsler-Reya and Scott, 2001). Members of the hedgehog family in mammals include Indian, Desert and Sonic hedgehog (Shh). In development, loss of hedgehog signaling results in severe abnormalities in mice and humans (Chiang et al., 1996). Conversely, unrestrained hedgehog pathway activation is implicated in a variety of tumors, many of which can be traced to hedgehog-dependent progenitors (Beachy et al., 2004; Eberhart, 2008; Teglund and Toftgard, 2010). Tumors associated with Hh aberrations comprise cancers of the skin, pancreas, lung, and the brain cancer medulloblastoma (Teglund and Toftgard, 2010; Wetmore, 2003), the most common solid malignant pediatric tumor, and a leading cause of cancer deaths in children. Medulloblastoma arises in the cerebellum as a result of aberrant activity of developmentally critical signaling pathways, including those activated by wnt, Notch, and Shh. Of note, Shh mitogenic signaling is required for normal cerebellum development (Dahmane and Ruiz-i-Altaba, 1999; Wechsler-Reya and Scott, 1999), which is marked by a brief period of rapid proliferation of Cerebellar Granule Neuron Precursor cells (CGNPs), proposed to be cells of origin for certain genetically defined classes of medulloblastoma (Eberhart, 2008).

Secreted hedgehog proteins trigger downstream signaling through interactions with the tumor suppressor Patched (Ptc), a trans-membrane protein localized to lipid rafts (Karpen *et al.*, 2001) whose loss or inactivation is documented in many hedgehog-dependent human tumors. Indeed, loss of Ptc was first identified in Gorlin's Syndrome that predisposes patients to basal cell carcinoma and medulloblastoma (Hahn *et al.*, 1996; Johnson *et al.*, 1996). In the absence of Shh binding, Ptc inhibits the evolutionarily conserved pathway activated by another transmembrane protein, Smoothed (Smo) (Ho and Scott, 2002). Shh interaction with Ptc leads to dis-inhibition of Smo signaling and consequent activation of Smo target genes following translocation from the cytoplasm to the nucleus of Gli transcription factors. Mammals possess three Gli family members, which have activator and repressor functions and are orthologous to *Drosophila* cubitus interruptus (Hepker et al., 1997). Gli1 and Gli2 primarily activate transcription in response to activated Smo signaling; in contrast, Gli3 serves to antagonize Shh signaling. In addition to *Gli1* and *Gli2*, other targets of Shh mitogenic signaling include the oncogenic transcriptional regulators *N-myc* and *YAP1*, the microRNA *miR17/92*, and members of the insulin signaling pathway such as IRS1, as well as *Ptc* itself, presumably as a negative feedback mechanism counteracting excessive Shh signaling (Fernandez et al., 2009; Kenney et al., 2003; Northcott et al., 2009; Oliver et al., 2003; Parathath et al., 2008; Platt et al., 1997; Uziel et al., 2009).

Notably, many diseases of cholesterol processing involve proteins that resemble Shh pathway components (i.e., Neiman-Pick syndrome (Incardona and Eaton, 2000)) or cause phenotypes reminiscent of hedgehog pathway malfunction (ie Smith-Lemli-Opitz syndrome (Kolf-Clauw et al., 1996)). Shh protein itself is modified by cholesterol and palmitoylation, and it has been reported that cholesterol plays downstream roles in Shh signaling (Corcoran and Scott, 2006). Nonetheless, negative effects of Shh on lipid biosynthesis have also been reported, underscoring the complexity of Shh signaling in the lipid regulatory process (Suh

et al., 2006). *In vivo*, an understanding of mechanisms through which Shh controls the metabolic machinery remains elusive and whether mitogenic Shh signaling alters lipogenic metabolic patterns to create a permissive environment for proliferation and tumor development is unknown. Nevertheless, many tumors exhibit exaggerated lipogenesis, a process that could fuel tumor growth through providing anabolic growth conditions and critical biomass accumulation, such as cell membrane components and other associated lipid molecules, including lipid rafts which themselves are essential for Shh signal transduction. (Karpen et al., 2001; Menendez, 2009).

Here, we demonstrate that Shh signaling is directly coupled to lipogenesis in Shh-dependent medulloblastomas and in proliferating CGNPs. We show that Shh promotes *de novo* fatty acid synthesis (FAS) concomitant with suppressing fatty acid oxidation (FAO) or 'fat burning'. Shh-regulated lipogenesis requires inactivation of the Rb/E2F1 tumor suppressor complex leading to the up-regulation of Fatty Acid Synthase (FASN), a key lipogenic enzyme over-expressed in many aggressive tumors (Menendez, 2009). Down-modulating E2F1 activity and/or E2F1-regulated lipid synthesis has profound negative effects on Shh-associated proliferation and medulloblastoma cell survival. These results provide insights into the etiology of cancer-associated metabolic patterns, demonstrate the functional link coupling the Rb-E2F1 tumor suppressor complex to the lipogenic/lipolytic balance, and underscore the role of Shh signaling in regulating the E2F1→FASN axis *in vivo*. Findings of this study could have broad implications in cancer, given that unrestrained hedgehog signaling and Rb pathway deregulation are widespread across the spectrum of human malignancies. These results will influence current treatment paradigms through exploring viable metabolic-based therapeutic modalities targeting E2F-regulated lipogenesis alone or in combination with modulators of E2F1 activity, particularly in contexts where Rb is inactivated or in hedgehog-associated tumors.

Results

Exaggerated lipogenesis in Shh-induced medulloblastomas coincides with Rb inactivation and E2F1 induction

NeuroD2-SmoA1 mice are transgenic for an activated mutant Smoothed allele driven by the *NeuroD2* promoter (Hatton et al., 2008). Approximately sixty percent of these mice develop medulloblastomas by six months of age. Exaggerated lipogenesis, indicative of active *de novo* lipid synthesis is detected in these tumors. Indeed, the tumors- unlike adjacent non-tumor cerebellar tissue- can be identified by a striking accumulation of large lipid droplets (as indicated by Oil Red O stain used to mark neutral lipids, Fig. 1A). Of note, recent studies from our lab have linked the expression of E2F1 or the inactivation of its negative regulator Rb to inhibition of glucose oxidation, a process typically associated with increased lipogenesis especially in pathological contexts such as obesity and diabetes (Hsieh et al., 2008). Indeed, *NeuroD2-SmoA1* medulloblastomas have high levels of phosphorylated (inactivated) Rb, accompanied by increased levels of E2F1 (Fig. 1B, 1C). E2F1 expression also correlates with levels of the lipogenic enzyme FASN (Fig. 1B, C) as well as the proliferation marker phosphorylated Histone H3. These results suggest that under Shh

pathway deregulation, aberrant E2F1 expression can be associated with priming the lipogenic machinery, potentially favoring a lipogenic phenotype in this Shh-driven cancer.

Shh increases levels of E2F1 and fatty acid synthesis in CGNPs

Above, we showed an association between Shh signaling and the Rb/E2F1→FASN axis in spontaneous medulloblastomas, proposed to arise from CGNPs (Eberhart, 2008), whose proliferation during perinatal development requires mitogenic signaling by Shh. To a large extent, primary cultures of CGNPs recapitulate the mitogenic signaling seen in the *NeuroD2-SmoA1* medulloblastomas. As shown in Figure 2A, pRb is phosphorylated in Shh-treated wild-type CGNPs (Fig. 2A) (Kenney and Rowitch, 2000). This phosphorylation was blocked by acute treatment with forskolin, which activates protein kinase A, a Shh pathway antagonist (Hammerschmidt et al., 1996), indicating that Rb phosphorylation occurs as a result of Shh pathway activation in proliferation-competent CGNPs.

Consistent with cdk-mediated Rb inactivation lying downstream of Shh signaling, increased levels of cdk2, cdk4, and cdk6 protein were detected in Shh-treated CGNPs, and correlated with increased activation of cdk2 as determined by *in vitro* immunoprecipitation kinase assays (Fig. 2B, C). These results predict that E2F proteins are activated in Shh-treated proliferating CGNPs, and indeed, increased levels of E2F1 (and E2F2, data not shown) protein and mRNA are seen in the presence of Shh (Fig. 2D, E). Of note, levels of E2F1 mRNA increased over time, suggesting that *in vitro*, Shh strongly promotes E2F protein activity, as E2F1 positively regulates its own expression (Johnson et al., 1994). E2F1 induction also corresponds to Shh signaling pathway activation as determined by *Gli1* expression in CGNPs treated with exogenous Shh (Fig. 2F). Importantly, Shh-treatment of CGNPs causes induction of the lipogenic enzyme *Acetyl CoA Carboxylase (ACC)* as well as *FASN*, consistent with the observations in *NeuroD2-SmoA1* medulloblastomas. Co-treatment with the Smoothed inhibitor cyclopamine (Berman et al., 2002) blocked Shh-mediated induction of *FASN*, *ACC* and *E2F1*. We next examined the levels of the Sterol Regulatory Element Binding Protein 1 (SREBP1), a master regulator of *FASN* transcription and whose activity and expression could be regulated in response to mitogens and nutrient sensors (Menendez and Lupu, 2007). As shown in Figure 2H, Shh stimulates levels of SREBP1 protein expression, both the precursor and cleaved (active) form as well as its mRNA expression (data not shown). Together, our findings thus far indicate that Shh signaling in proliferating primary neural precursors and medulloblastoma cells is associated with induction of *E2F1* and the *ACC*→*FAS* lipogenic axis, an effect that can be reversed by down-modulating Shh signaling.

Shh suppresses mitochondrial β -oxidation in CGNPs

Fatty acid oxidation is intimately coupled to FAS and the lipogenic process. To that extent, FAO and FAS are inversely linked: activation of one typically adversely influences the other (Dowell et al., 2005). A critical regulatory component of this balance lies in the activity of the aforementioned key enzyme *ACC* that modifies Acetyl-CoA into Malonyl-CoA, which is a potent inhibitor of mitochondrial β -oxidation and is also a substrate for *FASN* (Fig. 3A). We asked whether Shh-triggered *FASN* expression corresponds to reduced FAO capacities. First, we examined the expression of key FAO regulators, including *ACC*, as well as *ACO1*

and *MCAD*, two enzymes whose expression reflects enhanced FAO. Indeed, the Shh-induced *FASN* and *ACC* expression is accompanied by a reduction in *ACOX1* and *MCAD* levels, indicating a reduced overall FAO capacity in the presence of Shh (Fig. 3B). Notably, treatment of CGNPs with C75, a *FASN* inhibitor (Thupari et al., 2002), resulted in powerful suppression of *FASN* expression and corresponding induction of *ACOX1* and *MCAD* (Fig. 3B). This is consistent with reported effects of C75 on promoting FAO in cultured cortical neurons (Landree et al., 2004) and other cells (Kim et al., 2004; Loftus et al., 2000; Thupari et al., 2004). Next, we determined whether Shh functionally inhibits the rates of mitochondrial FAO in CGNPs. Palmitate oxidation was measured radiometrically to determine FAO rates as described (Djouadi et al., 2003). Indeed, Shh has a dramatic effect, significantly reducing FAO in primary CGNPs, compared to vehicle-treated CGNPs. Importantly, inhibiting Shh signaling with cyclopamine was sufficient to counteract the effect of Shh, restoring FAO rates almost to basal vehicle-control treated levels (Fig. 3C); cyclopamine alone had no effect on expression of *FAS* and FAO enzymes (Figure 2, Supplementary Figure 1). Taken together, these findings indicate that Shh impedes the mitochondrial β -oxidation machinery, in a manner reversible by an established inhibitor of Shh-mediated proliferation. Evidently, Shh signaling modulates the lipolytic/lipogenic balance in CGNPs, a process that is seemingly coupled to its mitogenic effects, likely through the activation of E2F1.

E2F1 is necessary for Shh-mediated proliferation and FAO suppression in CGNPs

Next, we took advantage of E2F1-deficient mice to address the requirement and/or contribution of E2F1 to Shh-regulated induction of *FASN* and the control of FAO in proliferating CGNPs. We analyzed protein lysates and histological sections from neonatal wild-type and age-matched E2F1^{-/-} mouse cerebella to characterize the relationship between E2F1 and *FAS*. A striking reduction of *FASN* protein as well as the proliferation marker cyclin D2 is found in E2F1-deficient cerebella (Fig. 4A, B), compared to wild-type counterparts. We also observed a reduction in SREBP1 levels in E2F1-deficient cerebella, consistent with the expression data in CGNPs. Nonetheless, levels of the cleaved enzyme were not significantly altered and it remains unclear at this stage whether a change in overall SREBP1 levels could explain the striking abrogation of *FASN* expression seen with E2F1 loss. Significantly, at post-natal day 7, the peak of CGNP proliferation *in vivo*, E2F1 and *FASN* localized to the external granule layer (EGL) in wild type pups, where CGNP proliferation takes place (Figure 4B, left and center panels). In contrast, the PN7 E2F1-null EGL has nearly undetectable *FASN* protein. These cerebella also exhibited strikingly reduced proliferation (phospho-Histone H3 staining Fig. 4B, center panels, 4C). As shown by hematoxylin and eosin staining (Fig. 4B), the PN7 E2F1^{-/-} EGL was reduced in thickness compared with that of age-matched wild-type controls. Reduced EGL thickness and diminished CGNP proliferation in the absence of E2F1 could underlie the observation that the E2F1-null adult cerebellum is hypoplastic (Cooper-Kuhn et al., 2002).

To confirm that reduced proliferation and diminished *FASN* levels in neonatal E2F1^{-/-} CGNPs was due to loss of E2F1 specifically in these cells and not a result of an earlier developmental defect, Shh-treated wild type CGNPs infected with lentiviruses carrying short hairpin (sh) RNAs targeting mouse E2F1 or a scrambled shRNA were evaluated. As shown

in Figure 4D, un-infected or scrambled shRNA-infected Shh-treated CGNPs have elevated E2F1, cleaved SREBP1 and FASN, in conjunction with increased proliferation as indicated by Rb phosphorylation and cyclin D2 elevation. Importantly, Shh-treated CGNPs also showed marked reduction in the levels of MCAD, consistent with Shh ability to suppress FAO and down-regulate *MCAD* mRNA expression as shown earlier (Figure 3B, 3C, and 4E). In contrast, E2F1 knockdown reduced levels of E2F1, as expected, as well as reduced levels of proliferation markers like phosphorylated Rb and cyclin D2. Importantly, E2F1 knockdown markedly blunts both SREBP1 and FASN protein levels and notably rescues MCAD expression. Consistently, E2F1 knock-down also reverses Shh-mediated FAO suppression (Fig. 4E). This is also consistent with the effect seen earlier with inhibition of Shh signaling with cyclopamine in CGNPs (Fig. 3). Thus, genetic ablation of E2F1 and *in vitro* lentivirus-mediated E2F1 knock-down reveal a requirement for E2F1 in Shh-mediated CGNP proliferation and FASN expression, concomitant with suppression of β oxidation and key associated markers like MCAD.

Inhibition of E2F activity or FA Synthase blocks Shh-associated medulloblastoma cell proliferation and viability *in vitro*

The requirement for Shh-driven E2F1-mediated lipogenesis in CGNP proliferation suggests that targeting E2F1 activity and lipid synthesis pathways could be effective in blocking Shh-induced medulloblastoma growth. Pzp53med cells were used to test the effects of E2F1 and lipogenesis inhibition on tumor cells. These cells were derived from a mouse *Ptc^{+/-}/p53^{-/-}* medulloblastoma and they have been used to model Shh mitogenic signaling (Berman et al., 2002; Corcoran and Scott, 2006). Treatment of Pzp53med cells with the cdk inhibitor roscovitine (10 nM) resulted in reduced levels of E2F1, FASN, Bmi1 [an E2F1 and Shh target (Leung et al., 2004; Nowak et al., 2006)], cyclin D2, cdk2, and cdk4 (Fig. 5A). This is associated with a cessation of proliferation as determined by quantification of phospho-histone H3 staining. Next we used C75, an inhibitor of FASN (McCullough et al., 2005; Thupari et al., 2002) shown to block lung tumor growth in mice (Orita et al., 2007; Orita et al., 2008). Treatment of these cells with C75, like roscovitine, significantly reduced proliferation (Fig. 5B). Moreover, western blot analysis reveals that while cdk inhibition, FASN inhibition, and the combination all result in reduced levels of the lipogenic enzyme FASN and proliferation markers, C75 potently induces cell death as suggested by increased levels of cleaved caspase 3 (Fig. 5C). This was confirmed by quantification of viability (Figure 5D); C75 synergized with increasing doses of roscovitine in driving Pzp53med cell death. Collectively, these findings indicate that, in these Shh-associated medulloblastoma cells where E2F1 is de-regulated, FASN activity is required for both proliferation and survival.

Cdk inhibition or counteracting lipogenesis reduces tumor growth and improves survival of Shh-driven medulloblastoma-bearing mice *in vivo*

The sensitivity of Pzp53med cells to cdk inhibition suggests a therapeutic potential for cdk inhibition in Shh-associated medulloblastomas *in vivo*. We therefore carried out a 2-week treatment regimen of the cdk inhibitor olomoucine (i.p., 3 mg/kg daily) or vehicle control on *NeuroD2-SmoA1*-transgenic mice bearing medulloblastomas as determined by symptomology (slight head tilt, minimal seizure), and magnetic resonance imaging. Ten

mice were used for each treatment. Olomoucine was used instead of roscovitine as dose escalation and toxicity studies (data not shown) indicated better brain penetration by this drug. Olomoucine treatment markedly extended survival of mice with medulloblastomas (Fig. 6A). Immunocytochemistry and western blotting revealed that olomoucine effectively reduced E2F1 levels, down-modulated cdk pathway activity, and impaired proliferation as indicated by reduced levels of PCNA, N-myc, and CyclinD2 (Fig.s 6B, C). An increase in cleaved caspase 3 in tumors of treated mice reflects an increase in the apoptotic index. A marked reduction in FASN levels with olomoucine is also detected consistent with reduced levels of E2F1 *in vivo*, and with results shown in Figure 4 and Figure 5.

We asked whether counteracting FASN-mediated lipogenesis would be sufficient to influence tumor pathophysiology *in vivo* and affect survival of medulloblastoma-bearing mice. First, we examined the effect of a short-term treatment regimen with the FASN inhibitor C75 (i.p., 30 mg/kg) on lipid accumulation. Medulloblastomas from drug-treated animals have no detectable neutral lipid staining, in contrast to the striking accumulation of lipid droplets in tumor-bearing vehicle-treated mice as determined by Oil Red O staining (Figure 7A). Western blot analysis of cerebella and medulloblastomas from vehicle or C75-treated mice also reveals reduced levels of FASN, consistent with abrogated *de novo* lipid synthesis as well as downmodulation of proliferation markers like cyclin D2, N-myc and cdk2 (Fig. 7B). Consistently, a marked reduction in mitosis as reflected by phospho-histone H3 quantification was observed in the tumors of C75-treated animals (Fig. 7C). Importantly, treatment of NeuroD2-SmoA1-tumor bearing mice with C75 promotes a remarkable increase in survival of these animals as compared to vehicle-treated tumor bearing counterparts (Figure 7D). Evidently, counteracting lipogenesis in Shh-driven medulloblastomas, like inhibition of Cdks, reduces tumor growth and improves survival *in vivo*. Together, our findings establish a connection, *in vivo* and *ex vivo*, between Shh mitogenic signaling and the E2F1→FAS axis. This link underscores the coupling between hedgehog-dependent proliferation and the regulation of lipogenic machinery, deregulation of which as shown here is a prominent feature in medulloblastoma.

Discussion

Shh mitogenic signaling is critical in normal development and its aberrant activity is implicated in a wide range of human cancers like medulloblastoma, basal cell carcinoma, lung and pancreatic cancers to name a few. A better understanding of the mechanisms through which excessive Shh signaling engages the cell cycle machinery and recruits metabolic pathways to promote uncontrolled proliferation would characterize the oncogenic networks involved in the biology of cancer and as such inform therapeutic modalities. This will also improve our comprehension of Shh function in normal development and cell growth. Here, we show -using *in vivo* and *ex vivo* analyses- that Shh mitogenic/oncogenic signaling is tightly coupled to the reprogramming of mitochondrial bioenergetics: Shh inhibits the process of fatty acid oxidation while driving increased fatty acid synthesis, an early critical step of lipogenesis to favor tumor growth.

The effects of Shh on regulating this fundamental aspect of lipid metabolism are observed in CGNPs *in vivo* during development as well as in primary cultures *in vitro*. Exaggerated *de*

novo lipid synthesis and intracellular lipid accumulation with striking pathological features similar to those observed in the diabetic heart or with hepatic steatosis also mark Shh-dependent (*NeuroD2-SmoA1*) medulloblastomas. Importantly, Shh signaling engages the Rb/E2F1 tumor suppressor complex, inactivating Rb and inducing E2F1, a process we found essential for the effect of Shh on the lipogenic/lipolytic balance. These findings provide new mechanistic insight into how the Rb/E2F1 complex contributes to Shh-dependent proliferation and medulloblastoma (Marino et al., 2000; Olson et al., 2007), in that E2F1 has a pivotal role integrating the cell cycle regulatory machinery with metabolic pathways essential for cell growth, downstream of Shh. These novel connections between Shh signaling, E2F1 activation, and mitochondrial reprogramming of cellular bioenergetics favoring lipogenesis have broad implications for the treatment of Shh-associated cancers: they present lipogenesis inhibitors as potentially effective pharmacological tools to counteract hyperproliferative signals in tumors, downstream of Shh signaling.

In proliferating CGNPs, Shh pathway activation stimulates expression of FASN and ACC in an E2F1-dependent manner, and suppresses FAO, concomitant with a marked reduction of FAO markers like MCAD and ACOX1. Similarly, high levels of E2F1 are expressed in conjunction with FASN in CGNPs occupying the EGL of the developing cerebellum during the peak of Shh-mediated CGNP proliferation. Moreover, loss of E2F1 blunts Shh-mediated proliferation and down-regulates expression of lipogenic markers, including FASN. These findings contrast with a report that Shh inhibits adipogenesis in *Drosophila* fat bodies and 3T3-L1 cells (Suh et al., 2006). In those studies, non-proliferating cells in which Shh signaling was activated showed reduced levels of lipid accumulation and reduced expression of adipogenic transcription factors. To the contrary, we find that FASN is highly expressed in tumors with activated Shh signaling, consistent with the highly lipogenic phenotype apparent in the tumors as shown in Figure 1 and Figure 7. The effects of Shh signaling on lipogenesis could be highly nuanced and may depend on the proliferation competency of the Shh-responsive cells. Nonetheless, active lipogenesis marks Shh-driven medulloblastomas *in vivo*, a process that can also be reversed using lipogenesis inhibitors.

Altered metabolic patterns are a hallmark of cancer cells. Many tumors have elevated glucose uptake and hexokinase activity, a feature associated with poor prognosis and exploited in diagnostic imaging techniques like FDG-PET (Jones and Thompson, 2009). Conversely, some positive regulators of proliferation are associated with reduced hexokinase activities and reduced glycolysis. For example, antisense-mediated cyclin D1 down-modulation has been shown to up-regulate glycolysis *in vivo*, by releasing hexokinase II from inhibition (Sakamaki et al., 2006). This reflects the complexity of the network underlying cancer associated metabolic patterns and underscores its heterogeneity. It is also established that many cancer cells rely heavily on glutaminolysis (DeBerardinis et al., 2007; Tong et al., 2009), a process linked to the activity of the myc oncogene (Gao et al., 2009; Wise et al., 2008). Tumor suppressors such as p53, PTEN, and LKB1 also influence key regulators of cellular metabolism (Jones and Thompson, 2009). Recently, Akt-dependent sterol response element binding protein (SREBP)-mediated FASN regulation has also been linked to survival of glioma cells with activating EGF receptor mutations (Guo et al., 2009a; Guo et al., 2009b). We detected increased levels of SREPB1 precursor and cleaved protein

in Shh-treated CGNPs, and loss of E2F1 *in vivo* and *in vitro* led to a reduction in SREPB1 levels. Whether SREPB1 is responsible for FASN induction in CGNPs remains to be seen; we note however that changes in Akt activity are not observed in Shh-stimulated CGNPs (Parathath et al., 2008), and indeed, EGF receptor levels are inversely correlated with Gli levels in human medulloblastomas (Ferretti et al., 2006), indicating that FASN expression may be induced in CGNPs and Shh-associated medulloblastomas through a novel, E2F1-regulated process.

E2F1 directly regulates genes involved in cell cycle regulation, nucleotide biosynthesis, DNA replication, as well as apoptotic targets including caspases and Apaf-1 (Abrahamowicz et al., 2001; Dynlacht et al., 1997; Helin et al., 1993; Lees et al., 1993; Nahle et al., 2002; Ren et al., 2002; Zhu et al., 1995). E2F1 can also promote genomic instability and contributes to cancer progression (Hernando et al., 2004), through induction of the mitotic regulator Mad2. Previously, we identified pyruvate dehydrogenase kinase 4 (PDK4), a key nutrient sensor and an inhibitor of pyruvate dehydrogenase (PDH), as a direct E2F1 target, establishing a crucial role for E2F1 in metabolic regulation of glucose oxidation proper (Hsieh et al., 2008). HIF1 α was also linked to the induction of another PDK family member (PDK1) and the inhibition of PDH activity (Kim et al., 2006). Herein, we demonstrate that the Rb/E2F1 axis acts downstream of Shh to control the expression of lipogenic enzymes, promote active lipogenesis, and fuel tumor growth in medulloblastoma. This further underscores the intimate link between excessive E2F1 activity and the priming of hyperproliferative metabolic patterns, during both normal development and in tumors.

Shh-stimulated CGNPs and Shh-induced medulloblastomas exhibit high levels of FASN, a key lipogenic enzyme. This is functionally linked to high levels of neutral lipid accumulation, as evidenced by striking Oil red O staining. Using both genetic and pharmacologic approaches, we demonstrate a requirement for E2F1 in expression of FASN and for sustained suppression of fatty acid oxidation in both normally proliferating CGNPs and tumor cells. This connection between E2F1 and the lipogenic/lipolytic balance highlights a novel aspect of E2F1 function in cell cycle regulation and tumor cell growth, in addition to its well-established roles in regulating cell cycle progression and apoptosis genes, and highlights that E2F1-regulated metabolic pathways play important role in its oncogenic function. Further, direct inhibition of FASN by C75 resulted in medulloblastoma cell death *in vitro* and increased survival of medulloblastoma-bearing mice, associated with reduced lipid synthesis and decreased proliferation in the tumors *in vivo*. These data suggest a selective advantage for Shh-associated tumor cells with active lipogenesis, to which they become “addicted”. The dependence of Shh-associated medulloblastomas on fatty acid synthesis may be exploited in therapeutic approaches aiming at counteracting *de novo* lipid synthesis downstream of Smoothed, and may reduce the side effects or surmount acquired resistance associated with targeting Smoothed itself (Kimura et al., 2008; Yauch et al., 2009). Moreover, given that hedgehog pathway activation and Rb inactivation mark the majority of human malignancies; our work may have broad implications for therapies targeting the inextricable coupling between cell cycle control and lipogenesis, especially in cancers with Rb and/or Shh pathway defects. Finally, findings of this study are equally

relevant to the pathophysiology of chronic diseases like obesity and diabetes, where lipid signaling and fatty acid oxidation are also dysregulated.

Materials and Methods

Animal Studies

All mouse work was carried out in compliance with the Weill Cornell Medical College and Memorial Sloan-Kettering Institutional animal care and use committee guidelines. Wild-type and *NeuroD2-SmoA1* mice bearing tumors (kindly provided by Jim Olson of Fred Hutchinson Cancer Research Center) were administered 10% DMSO (control), olomoucine at 3 mg/kg daily, or C75 at 30 mg/kg through intraperitoneal injection. E2F1-null mice were obtained from the Jackson Laboratory.

Cell culture

CGNP cultures were generated as previously described (Kenney et al., 2003). Where indicated, Shh (R&D Systems) was used at a concentration of 3 mg/mL, cyclopamine (R&D Systems) was used at 10 µg/ml, and C75 (Sigma) was used at 10 µg/ml. Pzp53med cells, generously provided by Matt Scott (Stanford) were grown in DMEM/1% FCS, supplemented with antibiotics. As indicated, these cells were treated with roscovitine (Sigma)(10 nM for 18 hours), or C75 compound.

Lentivirus production and infection—E2F1 shRNA and scrambled control lentivirus constructs were obtained from The RNAi Consortium library (Sigma). Each construct was transfected into Pzp53med cells, and western blotting was used to determine which shRNAs effectively and specifically targeted E2F1. These constructs were used to prepare lentiviruses. 293T cells, grown in 10% FBS DMEM medium, were transfected with E2F1 or scrambled control shRNA lentiviral vectors and MISSION© lentiviral packaging mix (Sigma) using Fugene 6 in serum-free OPTI-MEM medium. Lentiviral supernatants were collected 48 hrs post-transfection and filtered through a 0.45 µm filter, then pooled. For infection, Shh-treated CGNPs were exposed to the lentiviral supernatant for 4 hours. Control scrambled shRNA lentivirus constructs were used to determine specificity for E2F1 and to rule out off-target effects or non-specific results due to the process of virus infection. The lentiviruses were aspirated and replaced with serum free CGNP medium (above) containing Shh. The cells were lysed or fixed 48 hours post-infection.

RT-PCR

RNA was isolated using the TRIZOL (Invitrogen) reagent according to the manufacturer's protocol. RNA samples were resuspended in 35µL DEPC-treated water. cDNA was generated with SuperScript First-Strand Synthesis System for RT-PCR (Invitrogen) as per manufacturer's instructions. TaqMan Gene Expression Arrays (Applied Biosystems) using TaqMan custom designed MGB probes for N-myc and Cyclin D2 were performed in triplicate according to manufacturer's protocol on an ABI 7000 Sequence Detection System. Data was analyzed with ABI GeneAmp SDS software (Applied Biosystems). The average threshold cycle (C_T) was determined to quantify transcript levels, normalized against b-actin and the results reported as fold changes. Cyber-green RT-PCR primers were used to detect

E2F1 (5'CCAAATTCCTCAATTCTGGTG3', 5'CAGCGAGGTAAGTATGGTCA3'), Gli1 (5' TGGACAACCTGCAGGTAACACC, 5'AATCCGGTGGAGTCAGACC), ACC (5'CTAAACCAGCACTCCCGATT3', 5'ACTAGGTGCAAGCCAGACAT3'), FAS (5'GTCTGGAAAGCTGAAGGATCTC, 5'TGCCTCTGAACCACTCACAC3'), MCAD (5'GAAGGTTGAACTCGCTAGGC3', 5'GCTAGCTGATTGGCAATGTC3'), and ACOX (5'GTATAAACTCTTCCCGCTCCTG3', 5'CCAGGTAGTAAAAGCCTTCAGC3'), using a Biorad iCycler and companion software for analysis.

Western blotting

Protein extracts were prepared as previously described (Kenney and Rowitch, 2000). A total of 40 mg murine cerebella and medulloblastoma protein, or 30 mg CGNP protein were run on 8–12% SDS-polyacrylamide gels and transferred to a PVDF membrane (Millipore). The blots were incubated with primary antibodies in 3% BSA (in PBS-T) or 5% milk overnight in 4°C. Blots were washed three times and incubated with secondary antibodies in 5% milk in TBS-T for two hours in room temperature. After washing, the signals were developed using the enhanced chemiluminescence method (Amersham) and the membranes were exposed to Kodak Biomax film. Primary antibodies were: E2F1 (Cell Signaling), FASN (Cell Signaling), MCAD (Abcam), Phospho-Rb S608 and S720 (Cell Signaling), total Rb (Cell Signaling), SREBP1 (Cell signaling), cdk2 (M-2; Santa Cruz), cdk4 (C-22; Santa Cruz), cdk 6 (C-21; Santa Cruz), N-myc (C19, Santa Cruz), β -tubulin (Sigma) and cyclin D2 (M-20; Santa Cruz). HRP conjugated secondary antibodies were: goat anti-rabbit IgG (H+L) (Thermo Scientific) and donkey anti-mouse IgG (H+L) (Jackson Immuno Research).

Immunoprecipitation kinase assay

Protein lysates were prepared as described above. Kinase assays were carried out precisely as described (Sjostrom et al., 2005), using two hundred μ g of lysate. Antibodies used were: anti-Erk (9102, Cell Signaling Technology) and anti-Cdk2 (Santa Cruz, sc-163). Kinase substrates were: 1 mg histone H1 (Roche), 5 mg MBP (Upstate Biotechnology). Results shown are representative of experiments carried out in triplicate.

Immunostaining

CGNPs and Pzp53med cells were fixed in 4% PFA for 10 minutes. Cells were then washed with 1xPBS and permeabilized in 1% TritonX-100 for 5 minutes. Cells were blocked in 5% goat serum in PBS-T (1xPBS and 0.1% TritonX-100) for one hour in room temperature, washed once with 1xPBS, and then incubated with primary antibody in 2.5% goat serum (in PBS-T) overnight in 4°C. They were washed three times with 1xPBS and incubated with secondary antibody for two hours in room temperature, then washed and mounted in DAPI-containing mounting medium (Vector Labs).

Paraffin-embedded tissue slides were processed as previously described before incubation with primary antibodies (Bhatia et al., 2009). Primary antibodies used were: E2F1 (H-137; Santa Cruz), ACC (Cell Signaling), FAS (Cell Signaling), P-Histone H3 (Cell Signaling), cleaved caspase 3 (Cell Signaling), PCNA (Calbiochem). Secondary fluorescent-tagged antibodies were: Alexa Fluor goat anti-rabbit 488/594 (Invitrogen) and Alexa Fluor goat anti-mouse 488/594 (Invitrogen).

Image Capturing

Immunostaining performed on cultured cells or tissue sections was visualized using a Leica DM5000B microscope and images were captured with Leica FW400 software. For quantification of phospho-Histone H3 immunostaining, TIFF images of four random fields were taken for each experimental group using the 10X objective. The percentage of P-Histone-H3-positive cells over the total number of cells, as determined by DAPI staining, was calculated using Image Pro Plus software (MediaCybernetics).

Statistics

Statistical analysis of quantitative immunostaining was performed using one-way ANOVA followed by a two-tailed *t*-test for comparisons between groups. All results are given as mean±s.e.m. All *in vitro* experiments were performed at least three times with separate litters to confirm reproducibility and consistency.

Oil Red Staining

Oil red staining of *NeuroD2-SmoA1* medulloblastoma frozen sections was performed by the histology core in the department of Pathology and Laboratory Medicine in the Hospital for Special Surgery and by the microcytometry core facility at Memorial Sloan Kettering Cancer Center according to established protocols.

FAO assay

Radiometric palmitate oxidation assays were carried out according to established methods (Djouadi et al., 2003). A reaction mixture was prepared by adding 60 µCi of [9,10(n)-³H]-palmitic acid to 2 mL of 10mM unlabeled palmitic acid in absolute ethanol. After complete evaporation of the solvent, the fatty acid was resuspended in 12 mL DMEM containing 3% fatty acid-free BSA and incubated at 4 C overnight. The reaction mixture was further diluted with DMEM to a final concentration of 100 µmol/L palmitic acid. Cells were plated in 12 well plates. After overnight incubation, the monolayer cultures, at 90–100% confluency, were washed with phosphate-buffered saline before addition of 300 µL of the reaction mixture. The cultures were then incubated at 37 C for 2 h. At the end of the incubation, the reaction mixture was removed and added to a solution of 10% Trichloroacetic acid followed by centrifugation at 4000g at 4 C for 10 min. The supernatant is then neutralized with 6M NaOH and transferred to ion exchange resin columns (DOWEX1x2-400, Sigma) for separating ³H₂O from the unreacted substrate. The eluates, containing ³H₂O, were collected into scintillation counting vials. After the columns were rinsed twice with 1.5 mL deionized water, 5 mL scintillant was added to each vial, and the samples were counted with a Beckman LS6500 scintillation counter. The reaction rate was expressed as (nmol [³H]FA/hr/cell number).

Viability assay

Cells were plated in 96-well plates at 90% confluence. Cell viability was assayed after 24hr of treatment with C75 and Roscovitine at the indicated concentrations using the CellTiter-Glo Luminescent Cell Viability Assay (Promega) as per manufacturer's instructions.

Supplementary Material

Refer to Web version on PubMed Central for supplementary material.

Acknowledgements

We thank Dr. Michael J. Klein and the Pathology and Laboratory Medicine group at the Hospital for Special Surgery and MSKCC microcytometry facility. We also thank Lori A. Mainwaring, Cedric Dray, Cemille Guldal, Elisa DeStanchina, and Fajun Yang for helpful discussions. These studies were funded by the Lung Cancer Center and the division of thoracic surgery at Weill Cornell Medical College (ZN), the NIH (NINDS R01NS061070) (AMK), and the Memorial Sloan-Kettering Brain Tumor Center (BB).

REFERENCES

- Abrahamowicz M, Grodzicky T, Li Y, Panaritis C, du Berger R, Cjte R, et al. APAF1 is a key transcriptional target for p53 in the regulation of neuronal cell death. *Arthritis & Rheumatism*. 2001; 44:2331–2337. [PubMed: 11665973]
- Beachy PA, Karhadkar SS, Berman DM. Tissue repair and stem cell renewal in carcinogenesis. *Nature*. 2004; 432:324–331. [PubMed: 15549094]
- Berman DM, Karhadkar SS, Hallahan AR, Pritchard JI, Eberhart CG, Watkins DN, et al. Medulloblastoma growth inhibition by hedgehog pathway blockade. *Science*. 2002; 297:1559–1561. [PubMed: 12202832]
- Bhatia B, Northcott PA, Hambarzumyan D, Govindarajan B, Brat DJ, Arbiser JL, et al. Tuberos Sclerosis Complex Suppression in Cerebellar Development and Medulloblastoma: Separate Regulation of Mammalian Target of Rapamycin Activity and p27Kip1 Localization. *Cancer Res*. 2009; 69:7224–7234. [PubMed: 19738049]
- Chiang C, Litingtung Y, Lee E, Young KE, Corden JL, Westphal H, et al. Cyclopia and defective axial patterning in mice lacking Sonic hedgehog gene function. *Nature*. 1996; 383:407–413. [PubMed: 8837770]
- Cooper-Kuhn CM, Vroemen M, Brown J, Ye H, Thompson MA, Winkler J, et al. Impaired adult neurogenesis in mice lacking the transcription factor E2F1. *Mol Cell Neurosci*. 2002; 21:312–323. [PubMed: 12401450]
- Corcoran RB, Scott MP. Oxysterols stimulate Sonic hedgehog signal transduction and proliferation of medulloblastoma cells. *Proc Natl Acad Sci U S A*. 2006; 103:8408–8413. [PubMed: 16707575]
- Dahmane N, Ruiz-i-Altaba A. Sonic hedgehog regulates the growth and patterning of the cerebellum. *Development*. 1999; 126:3089–3100. [PubMed: 10375501]
- DeBerardinis RJ, Mancuso A, Daikhin E, Nissim I, Yudkoff M, Wehrli S, et al. Beyond aerobic glycolysis: transformed cells can engage in glutamine metabolism that exceeds the requirement for protein and nucleotide synthesis. *Proceedings of the National Academy of Sciences of the United States of America*. 2007; 104:19345–19350. [PubMed: 18032601]
- Djouadi F, Bonnefont JP, Munnich A, Bastin J. Characterization of fatty acid oxidation in human muscle mitochondria and myoblasts. *Mol Genet Metab*. 2003; 78:112–118. [PubMed: 12618083]
- Dowell P, Hu Z, Lane MD. Monitoring energy balance: metabolites of fatty acid synthesis as hypothalamic sensors. *Annu Rev Biochem*. 2005; 74:515–534. [PubMed: 15952896]
- Dynlacht BD, Moberg K, Lees JA, Harlow E, Zhu L. Specific regulation of E2F family members by cyclin-dependent kinases. *Molecular & Cellular Biology*. 1997; 17:3867–3875. [PubMed: 9199321]
- Eberhart CG. Even cancers want commitment: lineage identity and medulloblastoma formation. *Cancer Cell*. 2008; 14:105–107. [PubMed: 18691544]
- Fernandez LA, Northcott PA, Dalton J, Fraga C, Ellison D, Angers S, et al. YAP1 is amplified and up-regulated in hedgehog-associated medulloblastomas and mediates Sonic hedgehog-driven neural precursor proliferation. *Genes Dev*. 2009; 23:2729–2741. [PubMed: 19952108]

- Ferretti E, Di Marcotullio L, Gessi M, Mattei T, Greco A, Po A, et al. Alternative splicing of the ErbB-4 cytoplasmic domain and its regulation by hedgehog signaling identify distinct medulloblastoma subsets. *Oncogene*. 2006; 25:7267–7273. [PubMed: 16878160]
- Gao P, Tchernyshyov I, Chang TC, Lee YS, Kita K, Ochi T, et al. c-Myc suppression of miR-23a/b enhances mitochondrial glutaminase expression and glutamine metabolism. *Nature*. 2009; 458:762–765. [PubMed: 19219026]
- Guo D, Hildebrandt IJ, Prins RM, Soto H, Mazzotta MM, Dang J, et al. The AMPK agonist AICAR inhibits the growth of EGFRvIII-expressing glioblastomas by inhibiting lipogenesis. *Proc Natl Acad Sci U S A*. 2009a; 106:12932–12937. [PubMed: 19625624]
- Guo D, Prins RM, Dang J, Kuga D, Iwanami A, Soto H, et al. EGFR signaling through an Akt-SREBP-1-dependent, rapamycin-resistant pathway sensitizes glioblastomas to antilipogenic therapy. *Sci Signal*. 2009b; 2:ra82. [PubMed: 20009104]
- Hahn H, Wicking C, Zaphiropoulos PG, Gailani MR, Shanley S, Chidambaram A, et al. Mutations of the human homolog of *Drosophila* patched in the nevoid basal cell carcinoma syndrome. *Cell*. 1996; 85:841–851. [PubMed: 8681379]
- Hammerschmidt M, Bitgood MJ, McMahon AP. Protein kinase A is a common negative regulator of Hedgehog signaling in the vertebrate embryo. *Genes Dev*. 1996; 10:647–658. [PubMed: 8598293]
- Hatton BA, Villavicencio EH, Tsuchiya KD, Pritchard JI, Ditzler S, Pullar B, et al. The Smo/Smo model: hedgehog-induced medulloblastoma with 90% incidence and leptomeningeal spread. *Cancer Res*. 2008; 68:1768–1776. [PubMed: 18339857]
- Helin K, Wu CL, Fattaey AR, Lees JA, Dynlacht BD, Ngwu C, et al. Heterodimerization of the transcription factors E2F-1 and DP-1 leads to cooperative trans-activation. *Genes & Development*. 1993; 7:1850–1861. [PubMed: 8405995]
- Hepker J, Wang QT, Motzny CK, Holmgren R, Orenic TV. *Drosophila cubitus interruptus* forms a negative feedback loop with patched and regulates expression of Hedgehog target genes. *Development*. 1997; 124:549–558. [PubMed: 9053330]
- Hernando E, Nahle Z, Juan G, Diaz-Rodriguez E, Alaminos M, Hemann M, et al. Rb inactivation promotes genomic instability by uncoupling cell cycle progression from mitotic control. *Nature*. 2004; 430:797–802. [PubMed: 15306814]
- Ho KS, Scott MP. Sonic hedgehog in the nervous system: functions, modifications and mechanisms. *Curr Opin Neurobiol*. 2002; 12:57–63. [PubMed: 11861165]
- Hsieh MCF, Das D, Sambandam N, Zhang MQ, Nahle Z. Regulation of the PDK4 isozyme by the Rb-E2F1 complex. *Journal of Biological Chemistry*. 2008; 283:27410–27417. [PubMed: 18667418]
- Incardona JP, Eaton S. Cholesterol in signal transduction. *Curr Opin Cell Biol*. 2000; 12:193–203. [PubMed: 10712926]
- Johnson DG, Ohtani K, Nevins JR. Autoregulatory control of E2F1 expression in response to positive and negative regulators of cell cycle progression. *Genes Dev*. 1994; 8:1514–1525. [PubMed: 7958836]
- Johnson RL, Rothman AL, Xie J, Goodrich LV, Bare JW, Bonifas JM, et al. Human homolog of patched, a candidate gene for the basal cell nevus syndrome. *Science*. 1996; 272:1668–1671. [PubMed: 8658145]
- Jones RG, Thompson CB. Tumor suppressors and cell metabolism: a recipe for cancer growth. *Genes Dev*. 2009; 23:537–548. [PubMed: 19270154]
- Karpen HE, Bukowski JT, Hughes T, Gratton JP, Sessa WC, Gailani MR. The sonic hedgehog receptor patched associates with caveolin-1 in cholesterol-rich microdomains of the plasma membrane. *J Biol Chem*. 2001; 276:19503–19511. [PubMed: 11278759]
- Kenney AM, Cole MD, Rowitch DH. Nmyc upregulation by sonic hedgehog signaling promotes proliferation in developing cerebellar granule neuron precursors. *Development*. 2003; 130:15–28. [PubMed: 12441288]
- Kenney AM, Rowitch DH. Sonic hedgehog promotes G(1) cyclin expression and sustained cell cycle progression in mammalian neuronal precursors [In Process Citation]. *Mol Cell Biol*. 2000; 20:9055–9067. [PubMed: 11074003]

- Kim EK, Miller I, Aja S, Landree LE, Pinn M, McFadden J, et al. C75, a fatty acid synthase inhibitor, reduces food intake via hypothalamic AMP-activated protein kinase. *J Biol Chem.* 2004; 279:19970–19976. [PubMed: 15028725]
- Kim JW, Tchernyshyov I, Semenza GL, Dang CV. HIF-1-mediated expression of pyruvate dehydrogenase kinase: a metabolic switch required for cellular adaptation to hypoxia. *Cell Metab.* 2006; 3:177–185. [PubMed: 16517405]
- Kimura H, Ng JM, Curran T. Transient inhibition of the Hedgehog pathway in young mice causes permanent defects in bone structure. *Cancer Cell.* 2008; 13:249–260. [PubMed: 18328428]
- Kolf-Clauw M, Chevy F, Wolf C, Siliart B, Citadelle D, Roux C. Inhibition of 7-dehydrocholesterol reductase by the teratogen AY9944: a rat model for Smith-Lemli-Opitz syndrome. *Teratology.* 1996; 54:115–125. [PubMed: 8987154]
- Landree LE, Hanlon AL, Strong DW, Rumbaugh G, Miller IM, Thupari JN, et al. C75, a fatty acid synthase inhibitor, modulates AMP-activated protein kinase to alter neuronal energy metabolism. *J Biol Chem.* 2004; 279:3817–3827. [PubMed: 14615481]
- Lees JA, Saito M, Vidal M, Valentine M, Look T, Harlow E, et al. The retinoblastoma protein binds to a family of E2F transcription factors. *Molecular & Cellular Biology.* 1993; 13:7813–7825. [PubMed: 8246996]
- Leung C, Lingbeek M, Shakhova O, Liu J, Tanger E, Saremaslani P, et al. Bmi1 is essential for cerebellar development and is overexpressed in human medulloblastomas. *Nature.* 2004; 428:337–341. [PubMed: 15029199]
- Loftus TM, Jaworsky DE, Frehywot GL, Townsend CA, Ronnett GV, Lane MD, et al. Reduced food intake and body weight in mice treated with fatty acid synthase inhibitors. *Science.* 2000; 288:2379–2381. [PubMed: 10875926]
- Marino S, Vooijs M, van Der Gulden H, Jonkers J, Berns A. Induction of medulloblastomas in p53-null mutant mice by somatic inactivation of Rb in the external granular layer cells of the cerebellum. *Genes Dev.* 2000; 14:994–1004. [PubMed: 10783170]
- McCullough LD, Zeng Z, Li H, Landree LE, McFadden J, Ronnett GV. Pharmacological inhibition of AMP-activated protein kinase provides neuroprotection in stroke. *J Biol Chem.* 2005; 280:20493–20502. [PubMed: 15772080]
- Menendez JA. Fine-tuning the lipogenic/lipolytic balance to optimize the metabolic requirements of cancer cell growth: Molecular mechanisms and therapeutic perspectives. *Biochim Biophys Acta.* 2009
- Menendez JA, Lupu R. Fatty acid synthase and the lipogenic phenotype in cancer pathogenesis. *Nat Rev Cancer.* 2007; 7:763–777. [PubMed: 17882277]
- Nahle Z, Polakoff J, Davuluri RV, McCurrach ME, Jacobson MD, Narita M, et al. Direct coupling of the cell cycle and cell death machinery by E2F. *Nat Cell Biol.* 2002; 4:859–864. [PubMed: 12389032]
- Northcott PA, Fernandez LA, Hagan JP, Ellison DW, Grajkowska W, Gillespie Y, et al. The miR-17/92 polycistron is up-regulated in sonic hedgehog-driven medulloblastomas and induced by N-myc in sonic hedgehog-treated cerebellar neural precursors. *Cancer Res.* 2009; 69:3249–3255. [PubMed: 19351822]
- Nowak K, Kerl K, Fehr D, Kramps C, Gessner C, Killmer K, et al. BMI1 is a target gene of E2F-1 and is strongly expressed in primary neuroblastomas. *Nucleic Acids Res.* 2006; 34:1745–1754. [PubMed: 16582100]
- Oliver TG, Grasfeder LL, Carroll AL, Kaiser C, Gillingham CL, Lin SM, et al. Transcriptional profiling of the Sonic hedgehog response: a critical role for N-myc in proliferation of neuronal precursors. *Proc Natl Acad Sci U S A.* 2003; 100:7331–7336. [PubMed: 12777630]
- Olson MV, Johnson DG, Jiang H, Xu J, Alonso MM, Aldape KD, et al. Transgenic E2F1 expression in the mouse brain induces a human-like bimodal pattern of tumors. *Cancer Res.* 2007; 67:4005–4009. [PubMed: 17483310]
- Orita H, Coulter J, Lemmon C, Tully E, Vadlamudi A, Medghalchi SM, et al. Selective inhibition of fatty acid synthase for lung cancer treatment. *Clin Cancer Res.* 2007; 13:7139–7145. [PubMed: 18056164]

- Orita H, Coulter J, Tully E, Kuhajda FP, Gabrielson E. Inhibiting fatty acid synthase for chemoprevention of chemically induced lung tumors. *Clin Cancer Res.* 2008; 14:2458–2464. [PubMed: 18413838]
- Parathath SR, Mainwaring LA, Fernandez LA, Campbell DO, Kenney AM. Insulin receptor substrate 1 is an effector of sonic hedgehog mitogenic signaling in cerebellar neural precursors. *Development.* 2008; 135:3291–3300. [PubMed: 18755774]
- Platt KA, Michaud J, Joyner AL. Expression of the mouse *Gli* and *Ptc* genes is adjacent to embryonic sources of hedgehog signals suggesting a conservation of pathways between flies and mice. *Mech Dev.* 1997; 62:121–135. [PubMed: 9152005]
- Ren B, Cam H, Takahashi Y, Volkert T, Terragni J, Young RA, et al. E2F integrates cell cycle progression with DNA repair, replication, and G(2)/M checkpoints. *Genes & Development.* 2002; 16:245–256. [PubMed: 11799067]
- Sakamaki T, Casimiro MC, Ju X, Quong AA, Katiyar S, Liu M, et al. Cyclin D1 determines mitochondrial function in vivo. *Mol Cell Biol.* 2006; 26:5449–5469. [PubMed: 16809779]
- Sjostrom SK, Finn G, Hahn WC, Rowitch DH, Kenney AM. The *cdk1* complex plays a prime role in regulating N-myc phosphorylation and turnover in neural precursors. *Dev Cell.* 2005; 9:327–338. [PubMed: 16139224]
- Suh JM, Gao X, McKay J, McKay R, Salo Z, Graff JM. Hedgehog signaling plays a conserved role in inhibiting fat formation. *Cell Metab.* 2006; 3:25–34. [PubMed: 16399502]
- Teglund S, Toftgard R. Hedgehog beyond medulloblastoma and basal cell carcinoma. *Biochim Biophys Acta.* 2010
- Thupari JN, Kim E-K, Moran TH, Ronnett GV, Kuhajda FP. Chronic C75 treatment of diet-induced obese mice increases fat oxidation and reduces food intake to reduce adipose mass. *American journal of physiology Endocrinology and metabolism.* 2004; 287:E97–E104. [PubMed: 14736702]
- Thupari JN, Landree LE, Ronnett GV, Kuhajda FP. C75 increases peripheral energy utilization and fatty acid oxidation in diet-induced obesity. *Proceedings of the National Academy of Sciences of the United States of America.* 2002; 99:9498–9502. [PubMed: 12060712]
- Tong X, Zhao F, Thompson CB. The molecular determinants of de novo nucleotide biosynthesis in cancer cells. *Curr Opin Genet Dev.* 2009; 19:32–37. [PubMed: 19201187]
- Uziel T, Karginov FV, Xie S, Parker JS, Wang YD, Gajjar A, et al. The miR-17~92 cluster collaborates with the Sonic Hedgehog pathway in medulloblastoma. *Proc Natl Acad Sci U S A.* 2009; 106:2812–2817. [PubMed: 19196975]
- Wechsler-Reya R, Scott MP. The developmental biology of brain tumors. *Annu Rev Neurosci.* 2001; 24:385–428. [PubMed: 11283316]
- Wechsler-Reya RJ, Scott MP. Control of neuronal precursor proliferation in the cerebellum by Sonic Hedgehog. *Neuron.* 1999; 22:103–114. [see comments]. [PubMed: 10027293]
- Wetmore C. Sonic hedgehog in normal and neoplastic proliferation: insight gained from human tumors and animal models. *Curr Opin Genet Dev.* 2003; 13:34–42. [PubMed: 12573433]
- Wise DR, DeBerardinis RJ, Mancuso A, Sayed N, Zhang XY, Pfeiffer HK, et al. Myc regulates a transcriptional program that stimulates mitochondrial glutaminolysis and leads to glutamine addiction. *Proc Natl Acad Sci U S A.* 2008; 105:18782–18787. [PubMed: 19033189]
- Yauch RL, Dijkgraaf GJ, Alicke B, Januario T, Ahn CP, Holcomb T, et al. Smoothed Mutation Confers Resistance to a Hedgehog Pathway Inhibitor in Medulloblastoma. *Science.* 2009
- Zhu L, Enders G, Lees JA, Beijersbergen RL, Bernards R, Harlow E. The pRB-related protein p107 contains two growth suppression domains: independent interactions with E2F and cyclin/cdk complexes. *EMBO Journal.* 1995; 14:1904–1913. [PubMed: 7743997]

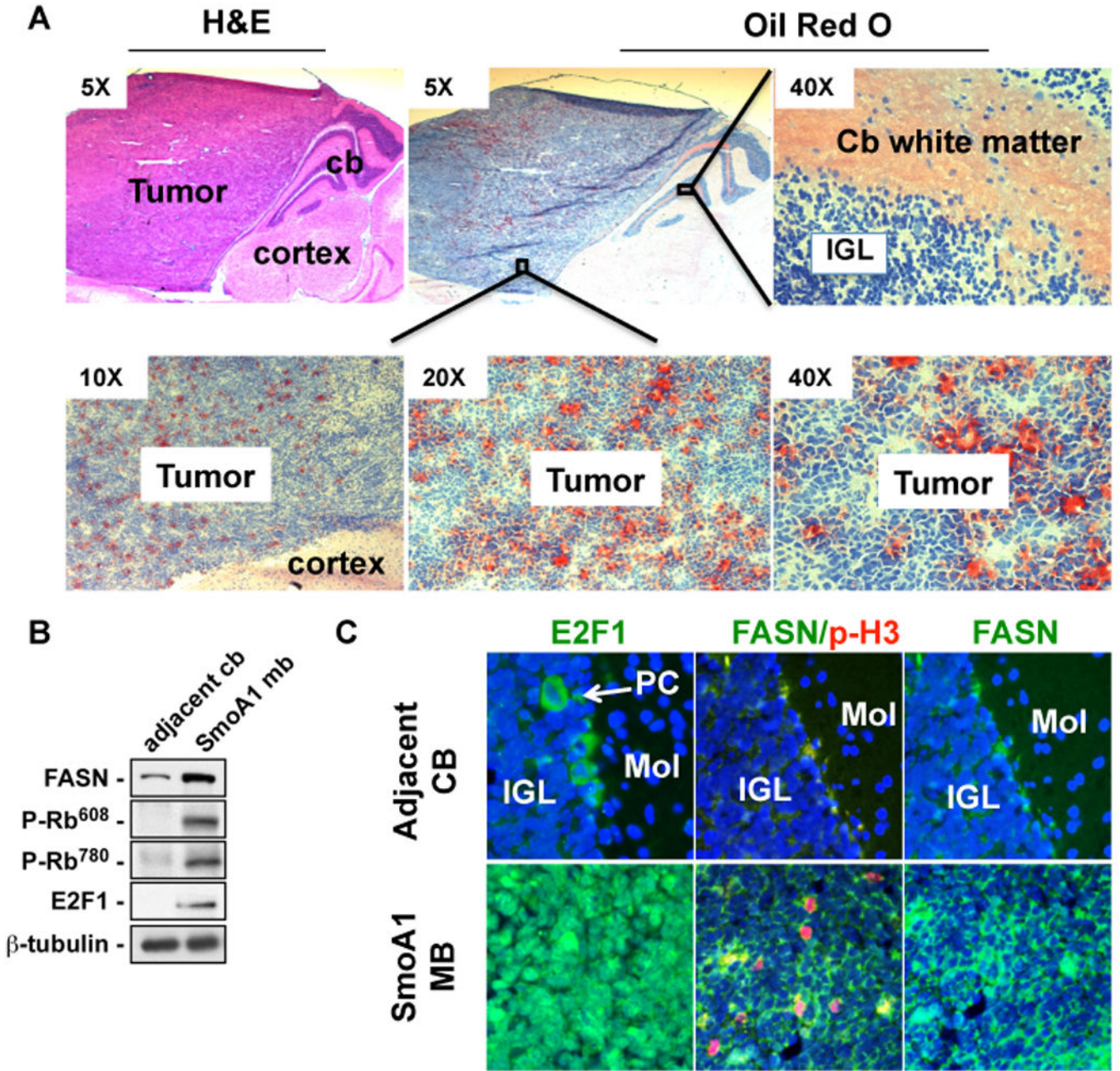


Figure 1. Shh-induced mouse medulloblastomas have exaggerated lipogenesis, increased levels of FASN, and deregulated E2F1

(A) Triglyceride accumulation was analyzed in a *NeuroD2-SmoA1* medulloblastoma using Oil Red O staining; lipids appear as red droplets. Upper row, leftmost panel shows H&E staining of the tumor and neighboring cortex and cerebellar white matter. (B) Protein lysates were prepared from *NeuroD2-SmoA1* normal cerebellum adjacent to the tumor, and tumor, then analyzed by western blotting for lipogenic markers (FASN) and proliferation markers (Rb phosphorylation, E2F1). 30 μg protein/lane was loaded. (C) *NeuroD2-SmoA1* medulloblastoma and adjacent non-tumor cerebellum were subjected to

immunofluorescence analyses for E2F1, FASN, and the proliferation marker phospho-histone H3.

Author Manuscript

Author Manuscript

Author Manuscript

Author Manuscript

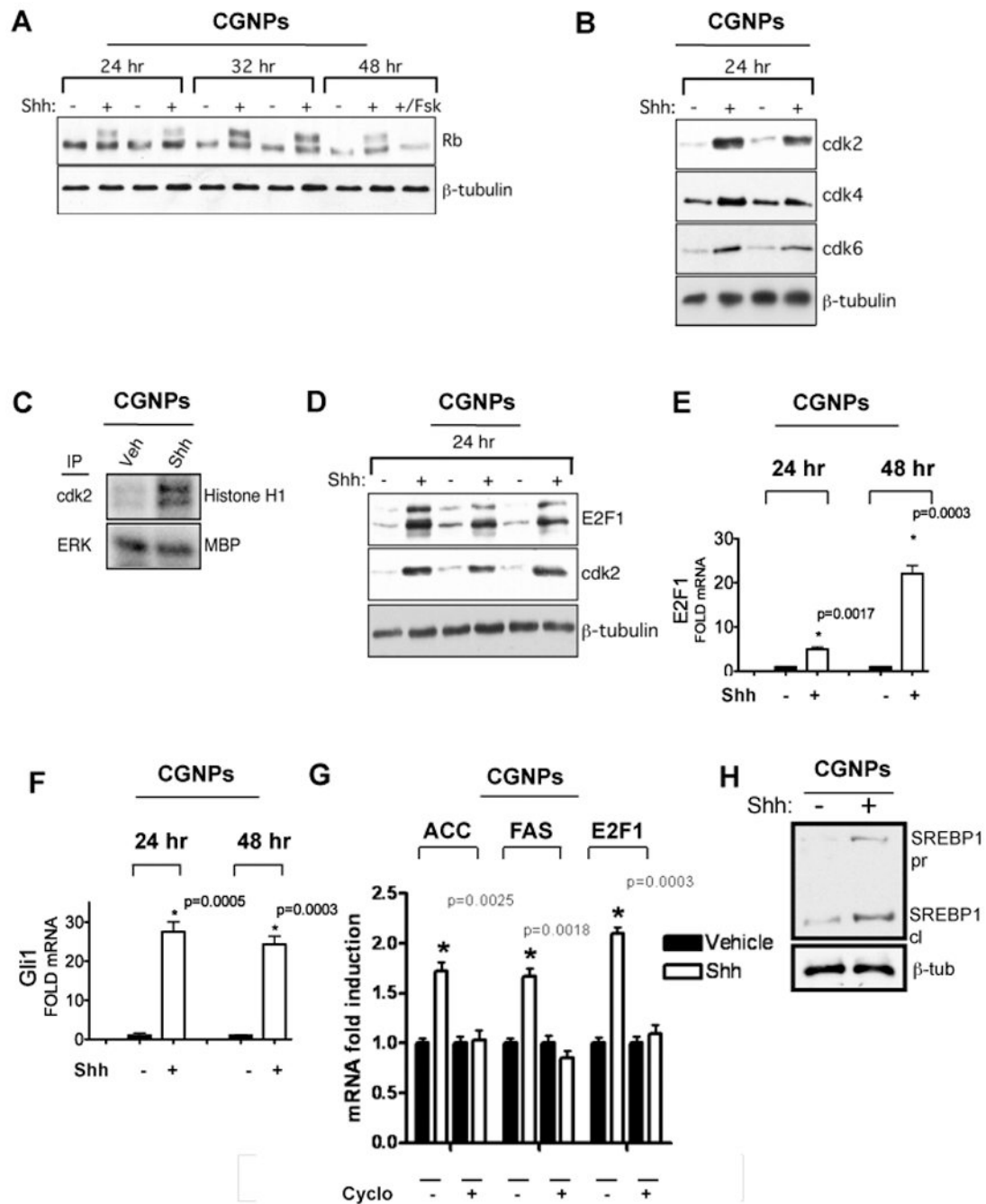


Figure 2. Shh signaling inactivates Rb and induces lipogenesis markers in primary CGNP cultures

(A) CGNP cultures were prepared from PN 4/5 mice and incubated with vehicle, Shh (3 μ g/mL), and/or forskolin (10 μ M) for up to 48 hours. Protein lysates were prepared and assayed for Rb phosphorylation as determined by upward mobility shift of the total protein. 50 μ g protein/lane were loaded. (B) CGNP cultures were treated with vehicle or Shh (3 μ g/mL) for 24 hours, then analyzed for levels of cdk 2, cdk 4, and cdk 6. (C) CGNP cultures prepared and treated as described above were analyzed for cdk2 kinase activity using immune

complex kinase assays. In brief, 200 μg protein lysate were incubated with protein A sepharose beads bound with antibodies against cdk2 or p48 MAPK, whose levels of activity are known not to be altered by Shh signaling. Beads were collected by centrifugation, washed, and incubated with substrate (cdk 2, Histone H1; p48 MAPK, myelin basic protein) in the presence of $\gamma\text{P}^{32}\text{-ATP}$. Reactions are separated by SDS page and visualized by exposure to X-ray film. Each radioactive (ie phosphorylated) substrate appears as a single band on the gel. (D) Western blot analysis of E2F1 levels in CGNPs treated with vehicle or Shh. (E) *E2F1* mRNA expression after 24 or 48 hours in CGNPs treated with vehicle or Shh, measured by quantitative RT-PCR. (F) Shh pathway activation as determined by qRT-PCR for *Gli1* mRNA expression in the same experiment shown in 1E. (G) CGNP cultures were treated with vehicle, Shh, or Shh and the Smoothened inhibitor cyclopamine (10 $\mu\text{g}/\text{mL}$). mRNA was prepared and analyzed by qRT-PCR for expression of *ACC*, *FASN*, and *E2F1*. (H) Western blot analysis of SREBP1 precursor (pr) and cleaved (cl) (active) form in CGNPs treated with vehicle or Shh.

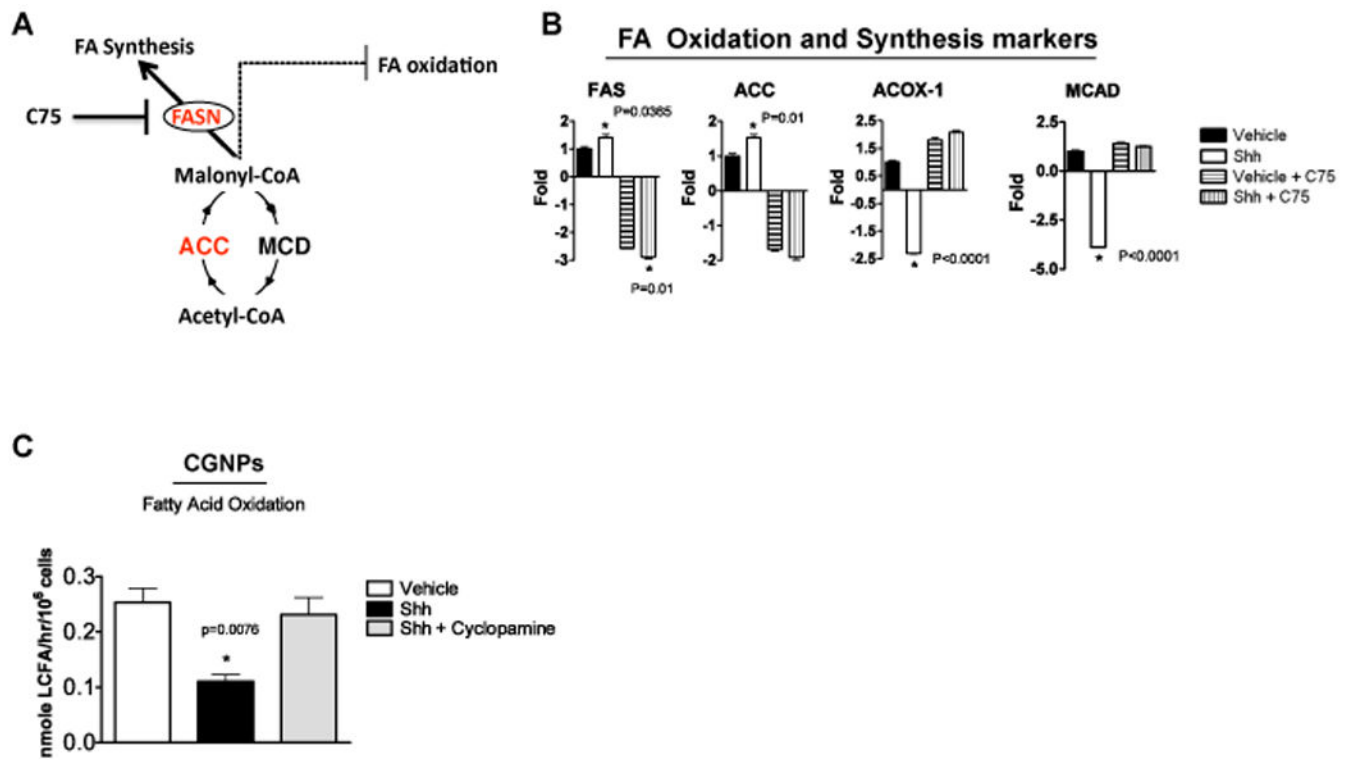


Figure 3. Pharmacological inhibition of FASN in Shh-treated CGNPs induces FAO-promoting enzymes while Shh itself reduces FAO rates

(A) Simple schematic demonstrating enzymes and substrates regulating the balance between FAS and FAO. The compound C75 inhibits the function of FASN. (B) CGNP cultures were treated with vehicle or Shh in the presence or absence of the FASN inhibitor C75 (10 $\mu\text{g}/\text{mL}$) for 48 hours. mRNA was prepared and analyzed by qRT-PCR for markers of FAS (*ACC*, *FASN*) or FAO (*ACOX1*, *MCAD*). (C) Quantification of radiometric analysis of FAO in CGNPs treated with vehicle or Shh in the presence or absence of cyclopamine. Briefly, after 48 hours in culture the CGNPs are exposed to H^3 -palmitate for 2 hours. After incubation, the level of $^3\text{H}_2\text{O}$, the byproduct of FAO, is measured and normalized to cell number/protein content, to generate a measurement of rate.

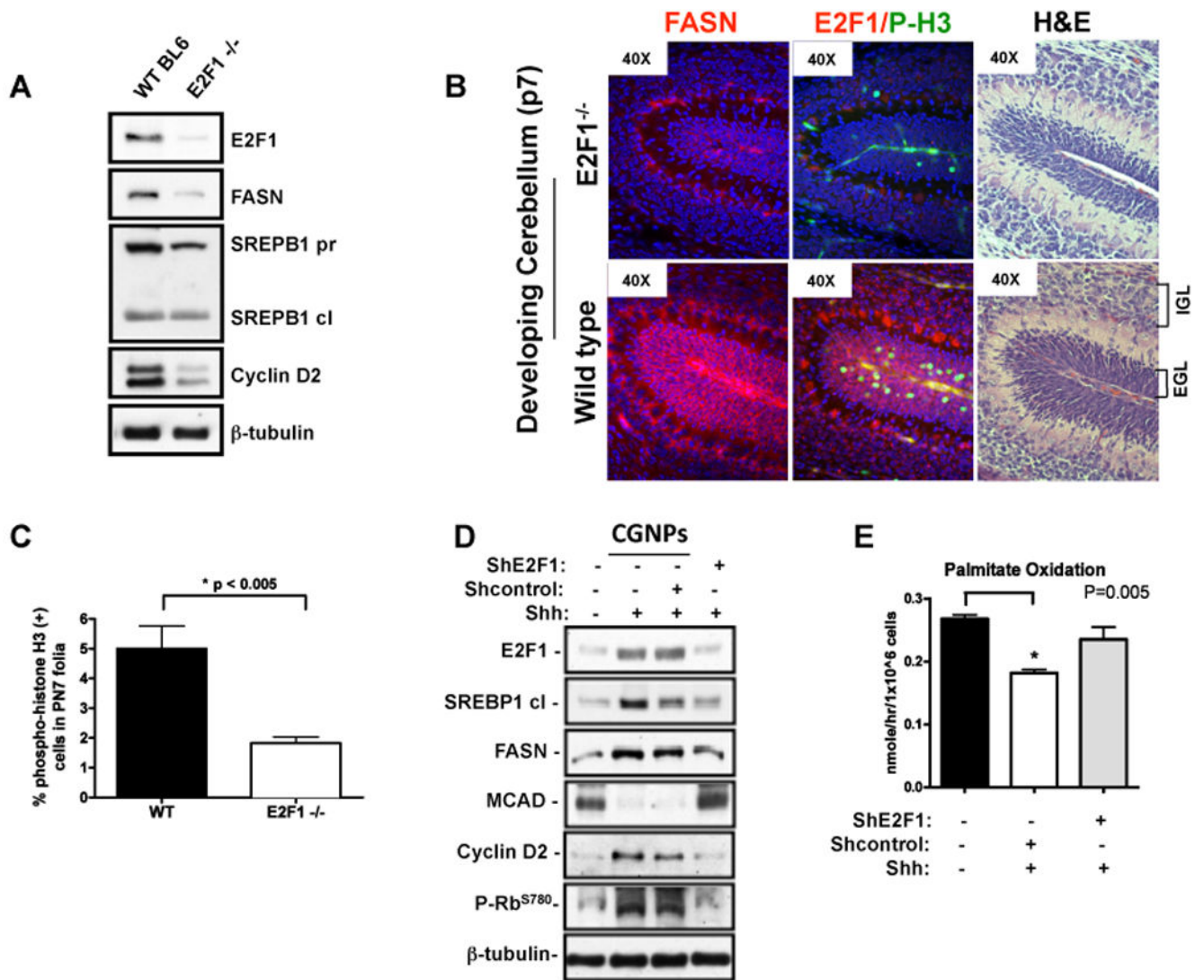


Figure 4. E2F1 is required for FASN expression, CGNP proliferation, and Shh-mediated FAO suppression

(A) Cerebella were collected from wild type or E2F1-null PN 5 pups, then analyzed by western blotting for levels of E2F1, lipogenic enzymes SREBP1 precursor and cleaved (active) form, and FASN, and the proliferation marker cyclin D2. (B) PN 7 sagittal sections of wild-type (bottom) and E2F1-null (top) cerebella were immunostained for FASN, E2F1, and phospho-histone H3. Rightmost panels show H&E staining. (C) Graph shows quantification of phospho-histone H3 staining as a measurement of proliferation. (D) Western blot analysis of E2F1, cleaved SREBP1, FASN, MCAD, and proliferation markers cyclin D2 and phospho-Rb in CGNPs treated with vehicle, Shh, or Shh in the presence of lentiviruses carrying shRNAs targeting E2F1 or a scrambled control shRNA virus. (E) Rates of FAO in CGNPs treated with vehicle, Shh+ scrambled control shRNA, or Shh+ shE2F1, determined by radiometric analysis.

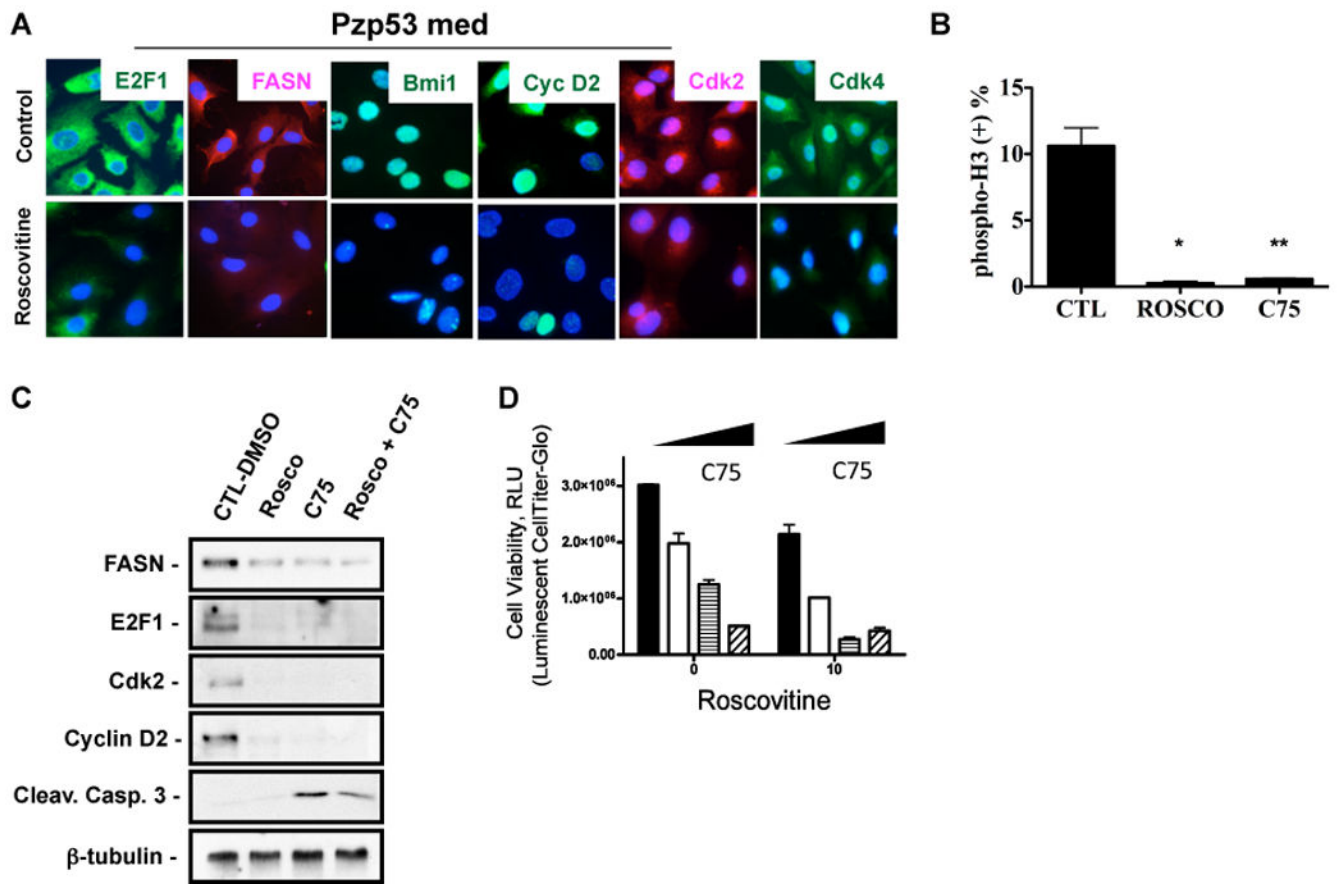


Figure 5. Inhibition of E2F1 and FASN is cytotoxic to medulloblastoma cells *in vitro*
 (A) Immunofluorescence analysis of E2F1, FASN, E2F1/Shh target Bmi1, cyclin D2, cdk 2, and cdk 4 in Pzp53med cells treated with DMSO (control) or the cdk inhibitor roscovitine (10 nM) for 18 hours. (B) Proliferation quantification in the presence of vehicle, cdk inhibitor roscovitine (10 nM), and FASN inhibitor C75 (10 μ g/ml) determined by counting phospho-histone H3-positive cells. (* p value = 0.0162; ** p value = 0.0188, t-test analysis) (C) Western blot analysis of proteins regulating lipogenesis (FASN), proliferation (E2F1, cdk2, cyclin D2), and apoptosis (cleaved caspase-3) in Pzp53med cells treated with roscovitine (10 nM), C75 (10 μ g/ml), or a combination of both drugs. (D) Effects of increasing doses of the FASN inhibitor C75 (0, 3, 10, 30 μ g/ml) in the presence of roscovitine, 0 or 10 nM, on Pzp53med cell viability as determined by cell Titer-Glo assay, a bioluminescent analysis which reports ATP concentration.

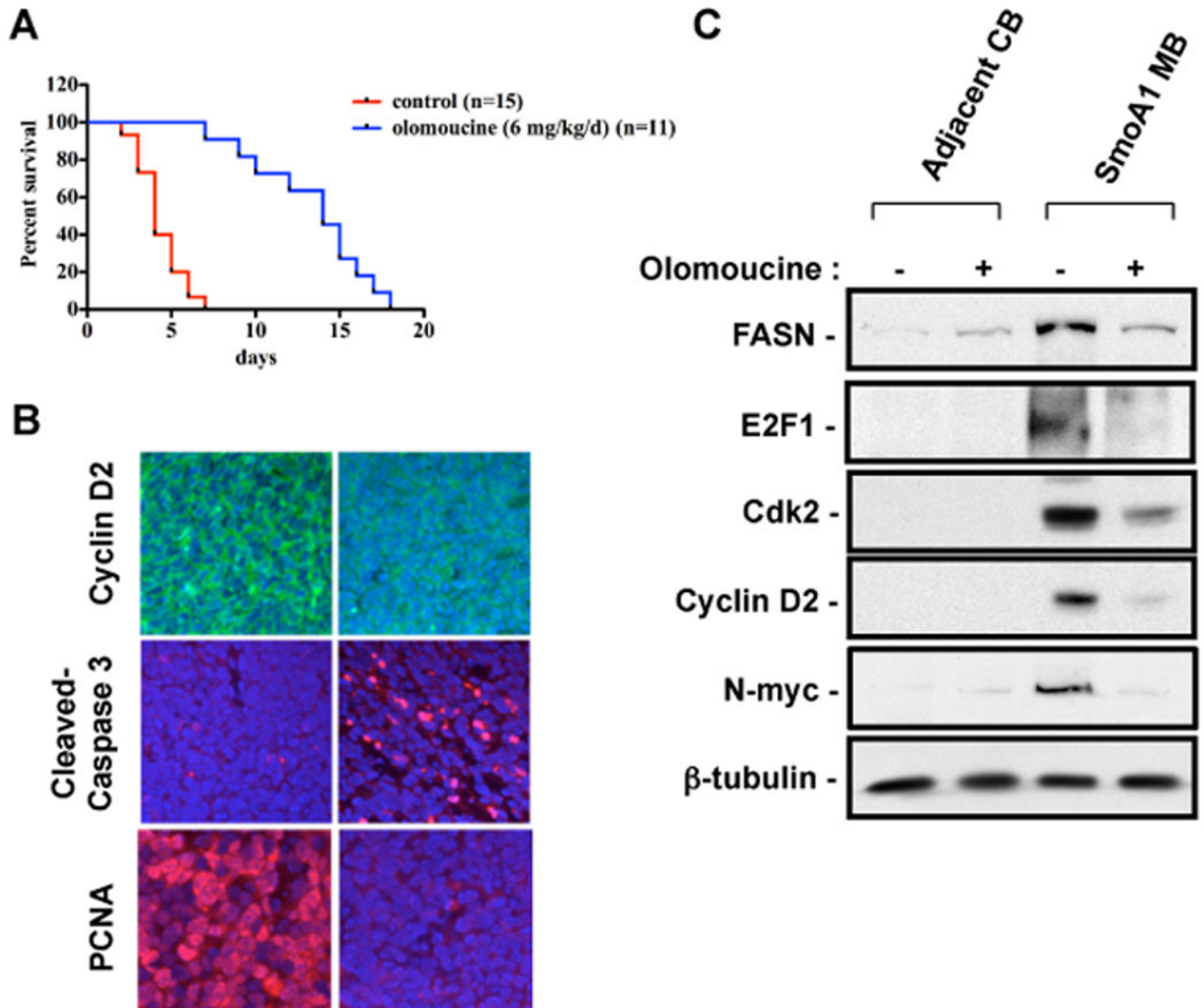


Figure 6. Inhibition of E2F1 is toxic to Shh-mediated medulloblastomas *in vivo* and reduces levels of FASN

(A) Kaplan-Meier survival curve of *NeuroD2-SmoA1* medulloblastoma-bearing mice in days commencing with initiation of treatment with DMSO or the cdk inhibitor olomoucine (6 mg/kg, i.p. injection daily) (* p value < 0.0001, Mantel-Cox test analysis). (B)

Immunofluorescence staining for markers of proliferation and survival in medulloblastomas collected from *NeuroD2-SmoA1* mice treated with DMSO (left column) or olomoucine (right column). (C) Western blot analysis of proteins regulating proliferation and lipogenesis in adjacent non-tumor cerebellar material or medulloblastomas from *NeuroD2-SmoA1* mice treated with DMSO (-) or olomoucine (+).

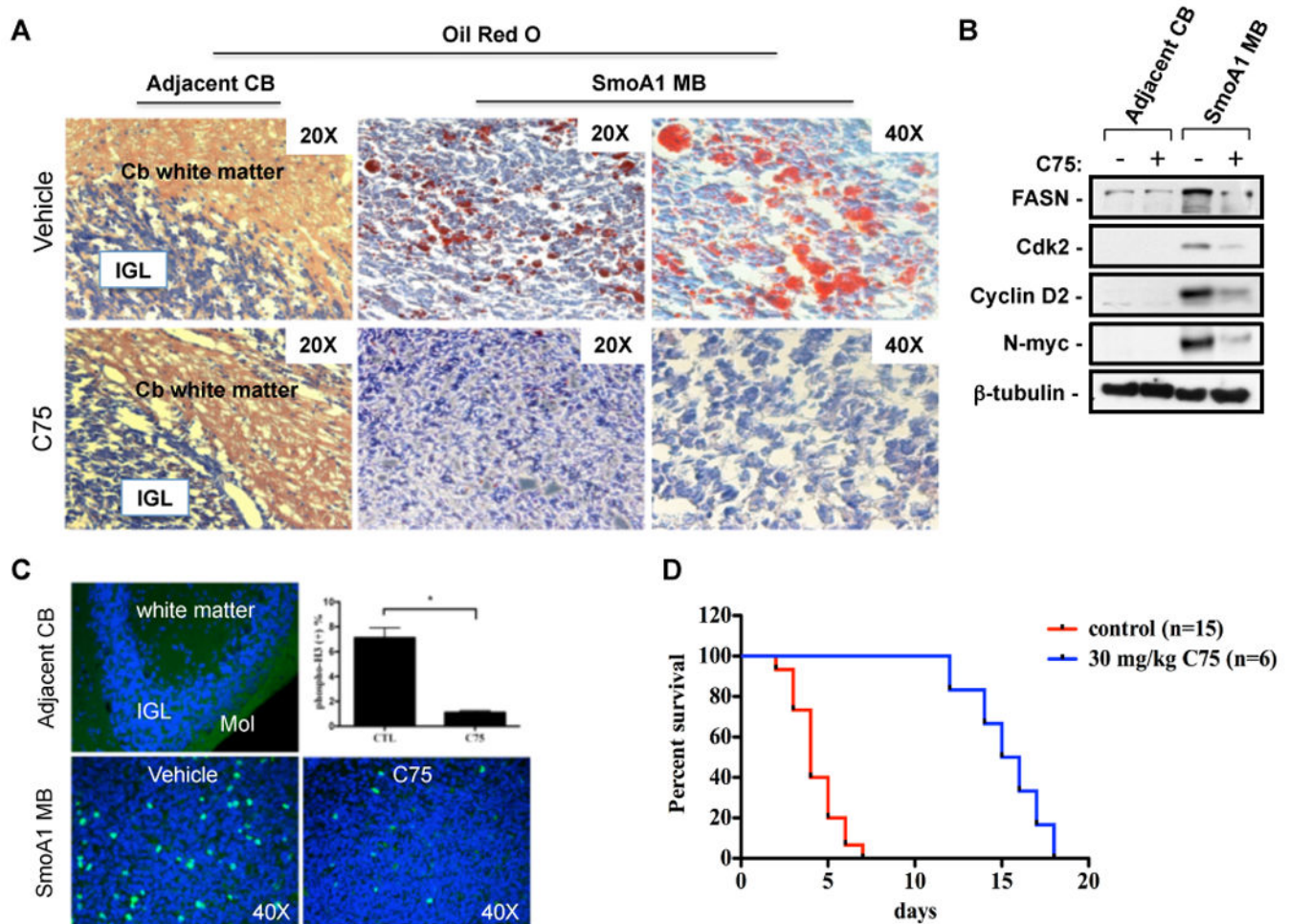


Figure 7. Treatment of medulloblastoma-bearing mice with FASN inhibitor C75 prolongs survival, reduces tumoral lipid accumulation, and impairs tumor cell proliferation *in vivo* (A) Oil Red O staining to mark neutral lipid accumulation in adjacent cerebellum and medulloblastomas of Vehicle (DMSO)-treated or C75-treated mice (30 mg/kg, i.p. injection 3 times a week). (B) Western blot analysis for markers of lipid synthesis (FASN) and proliferation (cyclin D2, N-myc, cdk2) in samples of adjacent cerebella and medulloblastomas from DMSO treated (-) or C75-treated (+) mice. (C) Immunostaining for phospho-histone H3 in adjacent cerebellum and medulloblastomas in vehicle- or C75-treated mice. Quantification of phospho-histone H3-positive (mitotic) cells is shown in the accompanying graph. (D) Kaplan-Meier survival curve of *NeuroD2-SmoA1* medulloblastoma-bearing mice in days commencing with initiation of treatment with DMSO or the FASN inhibitor C75 (* p value < 0.0001, Mantel-Cox test analysis).